Journal of Experimental Nanoscience
Publication details, including instructions for authors and subscription information:
http://www.informaworld.com/smpp/title~content=t716100757

Platinum tungsten oxide ($Pt\text{-}WO_3$) nanoparticles: their preparation in glycol and electrocatalytic properties

Kwok-Ying Tsang[a]; Tung-Chun Lee[a]; Jiawen Ren[a]; Kwong-Yu Chan[a]; Hengzhi Wang[b]; Huanting Wang[c]
[a] Department of Chemistry, The University of Hong Kong, Hong Kong, SAR, PR China [b] Department of Materials Science and Engineering, Nanjing University of Science and Technology, Nanjing 210094, China [c] Department of Chemical Engineering, Monash University, Clayton, VIC 3800, Australia

Online publication date: 28 September 2010

To cite this Article Tsang, Kwok-Ying , Lee, Tung-Chun , Ren, Jiawen , Chan, Kwong-Yu , Wang, Hengzhi and Wang, Huanting(2006) 'Platinum tungsten oxide ($Pt\text{-}WO_3$) nanoparticles: their preparation in glycol and electrocatalytic properties', Journal of Experimental Nanoscience, 1: 1, 113 — 123
To link to this Article: DOI: 10.1080/17458080500482297
URL: http://dx.doi.org/10.1080/17458080500482297

Journal of Experimental Nanoscience,
Vol. 1, No. 1, March 2006, 113–123

Taylor & Francis
Taylor & Francis Group

Platinum tungsten oxide (Pt–WO_3) nanoparticles: their preparation in glycol and electrocatalytic properties

KWOK-YING TSANG†, TUNG-CHUN LEE†, JIAWEN REN†, KWONG-YU CHAN*†, HENGZHI WANG‡ and HUANTING WANG§

†Department of Chemistry, The University of Hong Kong, Pokfulam Road, Hong Kong, SAR, PR China
‡Department of Materials Science and Engineering, Nanjing University of Science and Technology, Nanjing 210094, China
§Department of Chemical Engineering, Monash University, Clayton, VIC 3800, Australia

(*Received and in final form November 2006*)

A method to prepare supported nanoparticles of Pt–WO_3 with composition control in nanoscales is presented. Transmission electron microscopy shows crystal domains in the nanoparticles, which have a narrow size distribution. Energy dispersive X-ray analyses performed in different regions show good uniformity in the Pt : W ratio, which correlates linearly with the Pt : W ratio in the precursor. Platinum is mostly present in the pure metallic state whereas tungsten is in the +6 oxidation state, as revealed by X-ray photoelectron spectroscopy. The Pt–WO_3 nanoparticles supported on Vucan XC 72 carbon exhibit high activity for methanol oxidation at room temperature. The electrocatalytic activity varies with the Pt : W ratio with an optimum at 1 : 1. At this ratio, the activity is better than a commercial PtRu/C catalyst of equivalent platinum loading.

Keywords: Platinum–tungsten oxide; Methanol oxidation; Fuel cells; Pt–WO_3; Nanoparticles

1. Introduction

There has been a strong focus on the use of nanoparticles of metals, mixed metals, and metal oxides for catalysis in energy and environmental technologies. In the development of low-temperature fuel cells feeding on hydrogen or alcohols, platinum and platinum-based mixed metal nanoparticles are of particular interest. Nanoparticles of platinum mixed with other metal oxides are also effective and have received much attention. Efforts have been made to synthesize particles with uniform size and composition and to correlate activity to structural parameters. One of the objectives in industry has been to maximize the steady performance per unit mass of platinum. The second metallic co-catalyst, such as Ru, can also be expensive. A mini-review has been given recently on supported mixed metal nanoparticles for fuel cell catalysis [1]. A major problem in a direct methanol fuel cell (DMFC) or fuel cell feeding on impure hydrogen

*Corresponding author. Email: hrsccky@hku.hk

Journal of Experimental Nanoscience
ISSN 1745-8080 print/ISSN 1745-8099 online © 2006 Taylor & Francis
http://www.tandf.co.uk/journals
DOI: 10.1080/17458080500482297

is the poisoning of the catalyst surface by carbon monoxide, which is present as a reaction intermediate or an impurity. Binary and ternary platinum-based alloys like Pt–Ru [2], Pt–Mo [3], and Pt–Ru–Sn [4] have been investigated for their suitability as electro-oxidation of methanol and impure hydrogen. While Pt–Ru catalyst is currently considered to be the most effective anode catalyst for direct methanol fuel cells [5, 6], Pt–WO_3 [7] or Pt–Ru–WO_3 [8] has been a strong alternative. Pt–WO_3 has also shown unique activity for oxidation of glucose [9, 10]. The replacement of ruthenium by tungsten would also imply costs reduction and a lower barrier to commercialization.

Advances have been made in the synthesis of supported Pt–Ru nanoparticles with size and composition control [11, 12]. The same cannot be said for Pt–WO_3, which in turn also affects its competitiveness with Pt–Ru. A number of investigations on electrocatalytic properties of Pt–WO_3 were made in the past [7] but without refined control of the nanosize. Typically, Pt–WO_3 electrodes are prepared by a variety of techniques such as freeze drying [13], electrodeposition [14], and sputtering [15]. In these preparation methods, utilization of the catalysts is not optimized as large aggregates (150–200 nm) are commonly produced [7]. The preparation of nanoscopic metal colloids or metal nanoclusters has been intensively studied [16, 17]. For platinum and ruthenium, the common preparation involved the chemical reduction of their dissolved precursors to nucleate out into the metallic state. The glycol method [18], attractive for its simplicity and convenience in large-scale production, has been applied to prepare Pt–Ru nanoparticles [12]. Another alternative is the two-microemulsion technique [11, 19] in which particle size and composition are well controlled by the confinement of the microemulsion. While syntheses of WO_3 nanoparticles with organic ligands or water-in-oil microemulsions to synthesize WO_3 powder have been reported [20], the synthesis of Pt–WO_3 with good control of nanosize has not been reported. The difficulty lies in the difference in the types of reactions to deposit metal or metal oxide from its dissolved precursors. Platinum and ruthenium are both deposited by chemical reduction of precursors or decomposition of unstable precursors, whereas tungsten oxide is normally deposited from a tungstic acid precursor by a change in acidity without any change of oxidation state. Since tungsten is known to yield oxides of multiple oxidation states, acid–base precipitation without change of oxidation state is preferred to a redox reaction. In this paper, we report a simple approach to synthesizing Pt–WO_3 nanoparticles based on the glycol method. The final reaction step to precipitate WO_3 and Pt involves a sudden decrease in pH. The Pt–WO_3 nanoparticles have a narrow size distribution and a uniform composition. The electrocatalytic activities of Pt–WO_3 nanoparticles are studied for methanol oxidation. Their performance is correlated to the Pt : W ratio and compared with a commercial Pt–Ru catalyst.

2. Experimental

Colloidal platinum in ethylene glycol was prepared in a manner similar to previously reported [12, 18]. An ethylene glycol solution of $H_2PtCl_6 \cdot H_2O$ (5.6 mg mL^{-1}) was slowly added with stirring into a glycol solution of 0.5 M NaOH to obtain a

transparent yellow platinum colloidal solution. This mixture was then heated at 160°C for 3 h, with flowing N_2 to take away water vapour and organic by-products. A transparent dark-brown homogeneous colloidal solution of Pt was obtained without any precipitation. Previously reported syntheses of WO_3 nanoparticles used tungstic acid dissolved in water. Here, we replaced the solvent with ethylene glycol so that it is compatible with the glycol synthesis of platinum nanoparticles. Another solution of 0.05 M tungstic acid together with 0.5 M NaOH in ethylene glycol was prepared and Vulcan XC-72 carbon powder was immersed in this solution to adsorb the tungsten precursor. Excess 2 M HCl solution was then added to the tungsten impregnated carbon suspension and kept at 80°C for 5 h. Tungsten oxide precipitated according to the reaction

$$WO_4^{2-} + H^+ \longrightarrow WO_3 + H_2O. \quad (1)$$

The platinum colloidal solution was added afterwards and allowed to be adsorbed by the carbon and precipitated out in a period of 5 h. The $Pt–WO_3$ nanoparticle loaded carbon powder was collected by centrifugation and washed twice with ethanol. The amount of platinum precursor and tungsten precursor was predetermined and controlled. The dihydrogen hexachloroplatinate (IV) hydrate ($H_2PtCl_6 \cdot H_2O$) was supplied by Chempure Ltd and tungstic acid was supplied by Aldrich Chemical Company, Inc. Deionized water with 18.2 MΩ resistivity was produced by a Milli-Q ultrapure system. Organic solvents and other chemicals were analytical grade and used as received.

The $Pt–WO_3$ nanoparticles were characterized by a JOEL 2000FX transmission electron microscope (TEM). The TEM sample was prepared by placing 100 μL of a suspension of as-synthesized $Pt–WO_3$ nanoparticles onto a Holey® carbon coated copper TEM grid and let dry in a desiccator. Elemental analysis was obtained by a scanning electron microscope (Cambridge S360, UK) with an energy dispersion X-ray (EDX) analysis detector (Oxford Link eXL). Al Kα radiation at a base pressure below 5×10^{-9} torr provided the X-ray source for the X-ray photoelectron spectroscopy (XPS). The XPS spectra obtained were calibrated and corrected against the reference carbon peak line.

In the electrochemical experiments, an 8 mm diameter circular carbon electrode (area ~0.5 cm^2) was used as the support for the $Pt–WO_3$ nanoparticles. A suspension of as-synthesized $Pt–WO_3$ nanoparticles containing 0.1 mg Pt mL^{-1} was pipetted onto the surface of an ELAT carbon cloth electrode, supplied by E-TEK Inc., MA, USA. The loading of platinum was calculated by the amount of solution added to a known surface area of carbon electrode. When immersed into an aqueous electrolyte solution, the nanoparticles of the electrodes thus prepared did not redissolve and the electrolyte solution remained clear throughout. Electrochemical measurements were taken in a three-electrode electrochemical cell. A VOLTALAB 40 potentiostat from Radiometer and a BAS LG-50 galvanostat from Bioanalytical Systems Inc., USA, were used to control and record the current and voltage. The reference electrode was a Ag/AgCl saturated KCl electrode and methanol oxidation experiments were conducted in 0.5 M sulfuric acid.

3. Results and discussion

3.1. *Control of Pt : W ratio and uniformity of particle size*

Batches of Pt–WO_3 nanoparticles were prepared with different ratios of platinum and tungsten precursors as listed in table 1. Of each sample of unsupported Pt–WO_3 nanoparticles prepared, the resulting composition of the nanoparticles was analysed by EDX measurements on many different regions with analytical areas down to 100 nm in diameter. The Pt : W ratios in different regions are in close agreement without significant deviations. Table 1 gives the EDX results of Pt : W in the nanoparticles compared with the initial Pt : W ratio in the mixed precursors. The EDX results show that the nanoparticles have a higher Pt : W ratio in the initial precursor solutions. The precipitation of tungsten oxide by acid or the adsorption into carbon may not have been completed. This incomplete reaction, however, does not affect the control of the Pt : W ratio of the final product, which correlates linearly with the initial Pt : W ratio, as shown in figure 1. Figure 2(A) shows a typical TEM micrograph of the 1 : 1 Pt–WO_3 nanoparticles supported on Vulcan carbon. The sizes of 150 particles were measured to construct a histogram of particle size distribution in figure 2(B) with an average of

Table 1. Compositions of precursor solution versus EDX analyses of synthesized Pt–WO_3 nanoparticles.

Initial Pt : W in precursor	Pt : W in final Pt–WO_3 nanoparticle
1 : 0.83	1 : 0.32
1 : 2.5	1 : 1.12
1 : 5	1 : 2.01
1 : 7.5	1 : 3.04

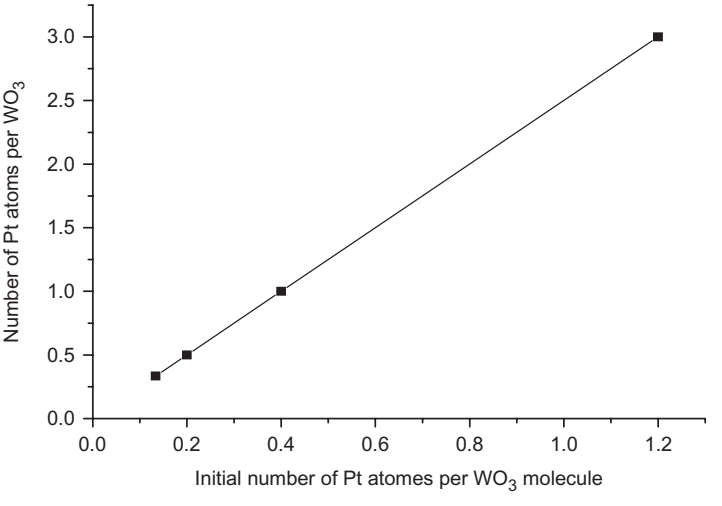

Figure 1. Correlation of Pt : W in precursor to Pt : W in the synthesized Pt–WO_3 nanoparticles.

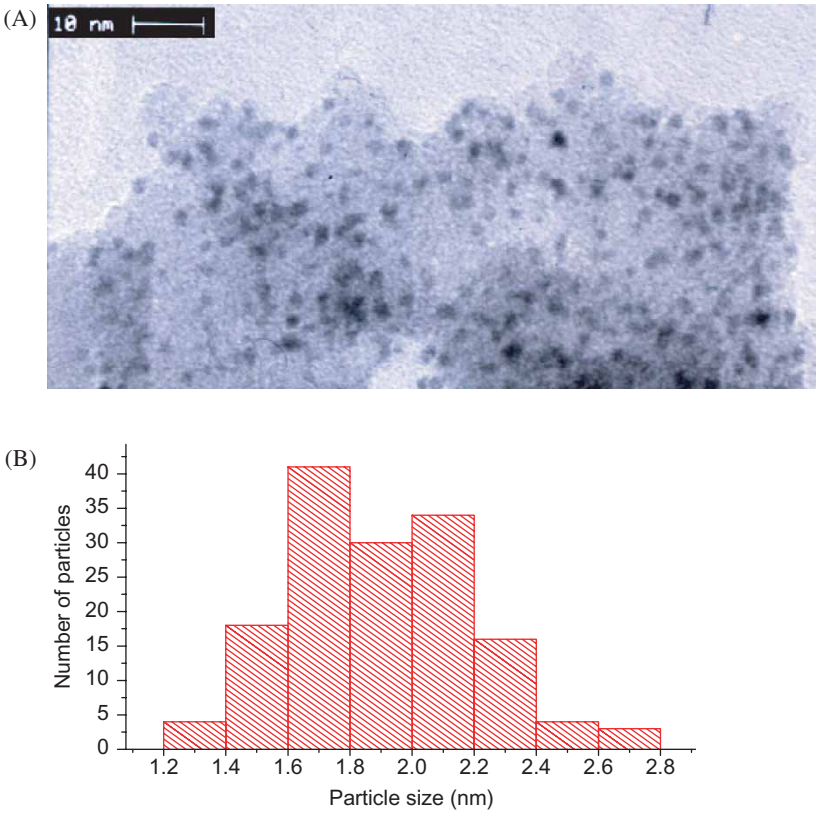

Figure 2. (A) TEM images of the as-synthesized $Pt–WO_3$ colloid catalysts (Pt : W ~ 1:1). (B) Histogram of particle size distribution for 150 $Pt–WO_3$ particles (Pt : W ~ 1 : 1). This figure is available in colour online.

1.9 nm diameter. A narrow size distribution is observed in the samples of all compositions and all samples have a similar average size. The glycol method thus offers good control of composition of metal–metal oxide nanoparticles while keeping a narrow size distribution and a small average size.

3.2. *Properties of $Pt–WO_3$ nanoparticles*

While the EDX results show uniform composition of Pt and W within an analytical region of 100 nm, it is uncertain whether Pt and WO_3 form a uniform alloy structure or a physical aggregate with different lattice domains. Pure platinum is a face centred cubic lattice with hexagonal lattice planes, whereas the WO_3 lattice is monoclinic with lattice planes {010} {103} forming a 2D rectangular pattern [21, 22]. It is also observed that Pt forms an fcc structure with Ru [11]. In the high-resolution TEM images of the $PtWO_3$ (1 : 1) shown in figure 3, crystalline lattice regions are observed, indicating the locations of metal or metal oxide. The {111} plane lattice space observed is 0.223 nm, compared roughly to the value of 0.227 nm in pure Pt. It is possible that the lattice

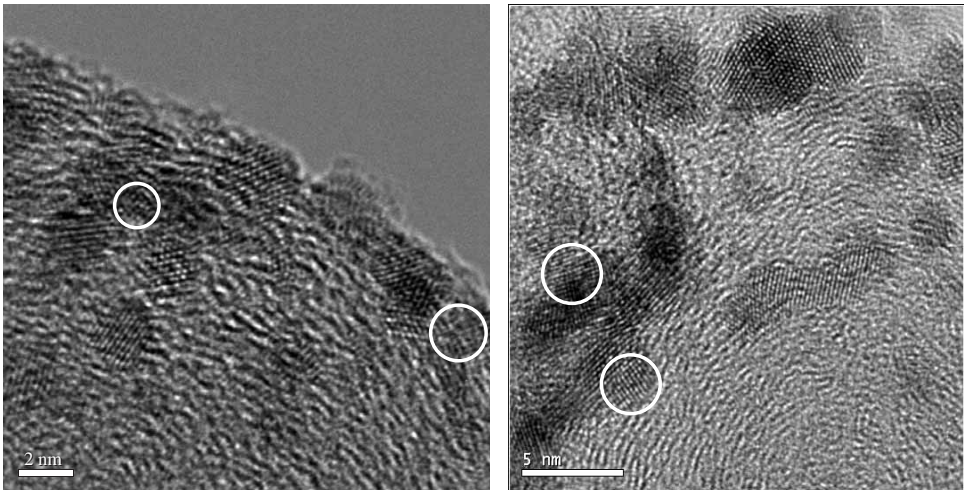

Figure 3. High-resolution TEM (HRTEM) images of the 1 : 1 Pt–WO_3 nanoparticles.

spacing is affected by the interpenetration of W and O atoms. Partial regions of square/rectangular lattice, however, can be observed, indicated the presence of WO_3 domains [21, 22]. This suggests some phase separation of Pt and WO_3 into adjacent domains of separate crystallinity. The penetration of W atoms into the Pt fcc lattice, however, cannot be ruled out. It has been observed that the interfaces of adjacent domains of Pt and Ru [23] and Pt–Ni [24] gives rise to good electrocatalytic activity for methanol oxidation. Therefore, $PtWO_3$ nanoparticles with separate but adjacent crystal lattice domains may be a desirable result.

Tungsten forms several stable oxides of different oxidation states. The acid precipitation of tungsten oxide from tungstic acid involves no redox reaction and the oxidation state of tungsten should remains as +6. The oxidation state of the metals in Pt–WO_3 nanoparticles was analysed by X-ray photoelectron spectroscopy (XPS) analyses. The test sample was supported on a carbon cloth electrode which will be the same as that used in the electrochemical experiments. Figure 4(A) shows the typical XPS spectra for the binding energies of Pt in the 1 : 1 Pt : WO_3 nanoparticles. The two peaks with binding energies of 70.75 eV and 74.08 eV correspond to Pt $4f_{7/2}$ and Pt $4f_{5/2}$ states of metallic Pt^0. There are minor discrepancies in the reference binding energy values of metallic Pt^0. Reference [25] gives 70.75 and 74.08 eV, whereas ref. [26] reports values of 71.2 and 74.53 eV. The Pt $4f_{5/2}$ peak has a shoulder region indicating the minor presence of platinum oxides. The values from ref. [15] are 72.95, 75.49 eV for Pt^{II} and 74.35, 77.47 eV for Pt^{IV}. Deconvolution of the peak yielded relative areas of integrated intensity of Pt^0, Pt^{II}, and Pt^{IV}, showing that the Pt in the nanoparticles was predominately metallic. The amounts of Pt^0, Pt^{II}, and Pt^{IV} are 77.7%, 18.2%, and 4.1%, respectively. Figure 4(B) shows the tungsten section of the XPS spectrum for the same 1 : 1 Pt–WO_3 nanoparticles. The doublet can be resolved into two peaks with binding energies at 35.5 eV for W $4f_{7/2}$ and 37.6 eV for W $4f_{5/2}$, respectively [27]. These peaks correspond to the +6 oxidation state of tungsten.

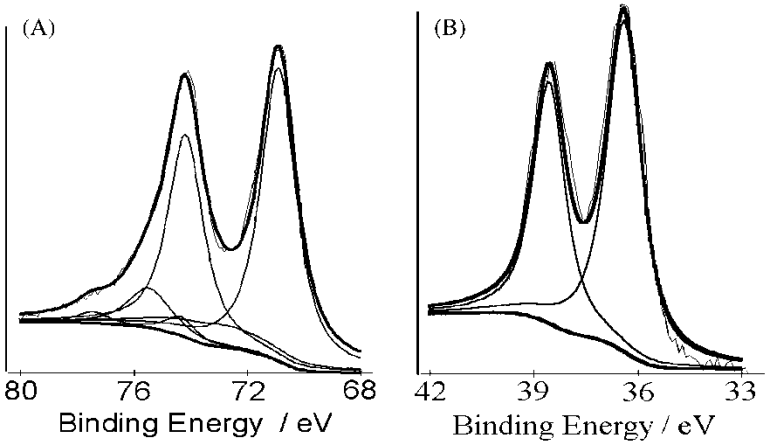

Figure 4. (A) The Pt 4f section of the XPS spectra for the sample with Pt : W ~ 1 : 1. The six deconvoluted peaks corresponding to Pt^0, Pt^{II}, Pt^{IV} are also shown. (B) The W4f section of the XPS spectra for the sample with Pt : WO_3 ~ 1 : 1. The two deconvoluted peaks corresponding to W $4f_{7/2}$ and W $4f_{5/2}$ are also shown. (The vertical scale is the intensity in arbitrary units.)

3.3. *Electrocatalytic activity of $PtWO_3$ nanoparticles and effect of Pt : W ratio*

We will focus on the electrocatalytic activity of $PtWO_3$ nanoparticles in methanol oxidation, which is the major reaction of concern for direct methanol fuel cells. The transient and steady-state oxidation of methanol are investigated by cyclic voltammetry, constant potential, and constant current electrochemical experiments. Comparison among nanoparticles of different Pt : W ratios and comparison with a commercial Pt–Ru catalyst were made on the basis of equal platinum metal loading. We prepared carbon cloth electrodes loaded with Pt–WO_3 nanoparticles of different Pt : W ratios, but with the same Pt loading of 10 μg Pt cm^{-2}. The Pt loading was about an order of magnitude lower than the US Department of Energy (DOE) targeted loading for commercial applications. This low loading was used in the transient voltammetry experiments for better differentiation of the activity of various Pt : W ratios and with the commercial catalyst. The experiments were performed in 0.5 M CH_3OH in 0.5 M H_2SO_4 electrolyte. The voltammograms after several initial cycles were recorded and are shown in figure 5 for the electrodes with different Pt : W ratios. In the potential region −0.2 V to 0.15 V, hydrogen adsorption and desorption peaks are observed. The oxidation of methanol commences near 0.378 V and reaches a peak at about 0.656 V. An anodic peak is observed in the reverse scan. The occurrence of reverse anodic peak is generally accepted as the reduction and regeneration of the platinum oxide formed during the forward scan. The characteristic parameters of the cyclic voltammograms (CV) of different electrodes are tabulated in table 2, showing the peak potential E_p, peak current density i_p, and the specific activity. The Pt : W ratio of 1 : 1 shows the highest peak current density of 1.2 A mg^{-1} of Pt, which is significantly better than a commercial 1 : 1 Pt–Ru electrode supplied from Etek, Inc. It should be noted that data on an electrode with a Pt : Ru electrocatalyst prepared similarly with control in size and composition should be available, before a conclusive comparison can

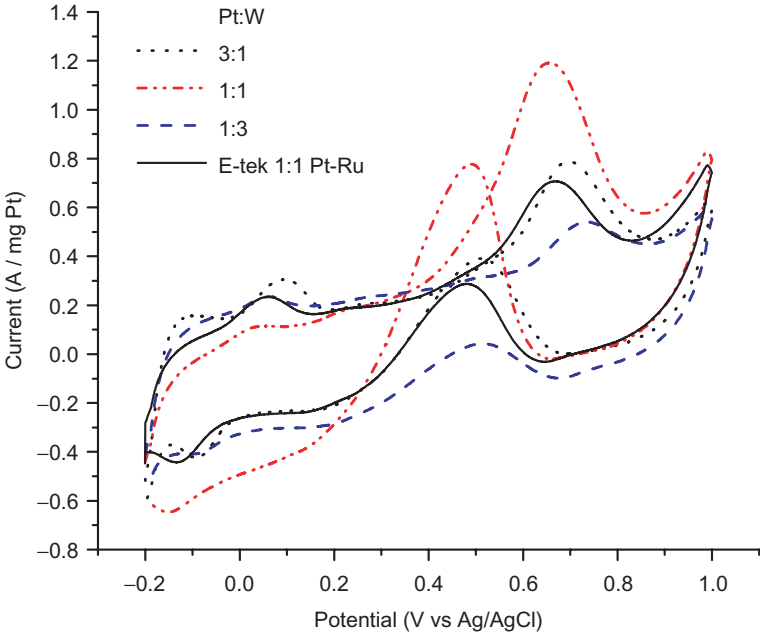

Figure 5. Cyclic voltammograms of the supported Pt–WO_3 nanoparticles of different Pt : W ratios in 0.5 M $CH_3OH + 0.5$ M H_2SO_4 at 25°C. (Scan rate is 50 mV s^{-1} and Pt loading is 10 μg Pt cm^{-2}.) This figure is available in colour online.

Table 2. Data from cyclic voltammograms (figure 5) of electrodes with different Pt : WO_3 ratios.

	Forward anodic peak		
Pt : W	E_p (V)	i_p (mA cm^{-2})	Specific activity (mA mg^{-1} of Pt)
1 : 0	0.682	2.11	476.86
3 : 1	0.696	3.52	795.52
1 : 1	0.656	5.38	1215.88
1 : 2	0.703	3.26	736.76
1 : 3	0.735	2.49	562.74
1 : 1 Pt : Ru (Etek)	0.670	3.13	707.38

be made. On the basis of equal platinum loading, the 3 : 1 Pt : W ratio gave similar activity to the 1 : 1 Pt : Ru Etek electrode, while the electrode with 1 : 3 Pt : W gave the lowest activity. The CV of the 1 : 2 Pt : W ratio was similar to that of 3 : 1 Pt : W ratio but for clarity, the curve was not included in figure 5. The role of WO_3 in promoting the oxidation of methanol had been discussed in light of the detailed reaction mechanism. A major factor has been the oxidation of the CO intermediate which can poison the platinum catalyst. It is therefore likely that an optimum ratio of Pt : W exists for the synergistic effect. Platinum is needed for the cleavage of C–H bonds, whereas WO_3 helps the oxidation of CO. Our results here support the optimum ratio of 1 : 1 Pt : W with nanoparticles prepared and characterized in the nanoscale. Several researchers have argued that the adjacent neighbourhood of the platinum and a

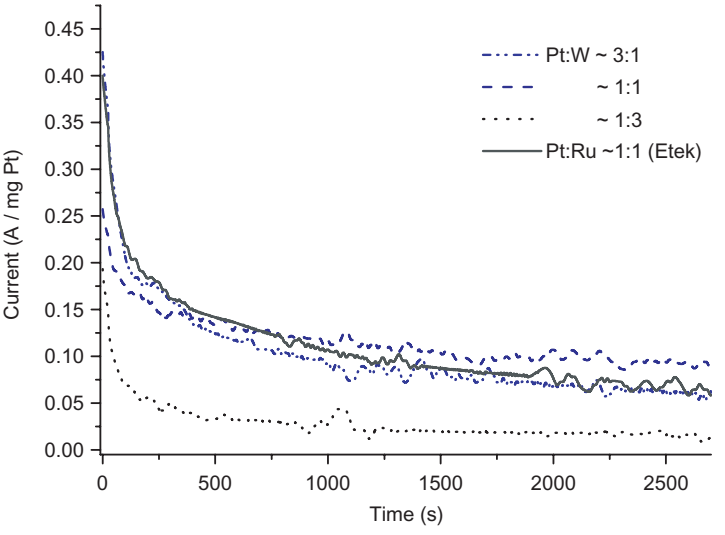

Figure 6. Comparison of different compositions of Pt–WO_3 catalysts for the electro-oxidation of 0.5 M CH_3OH + 0.5 M H_2SO_4 at 25°C at 0.65 V vs Ag/AgCl. (Pt loading is 10 μg Pt cm^{-2}.) This figure is available in colour online.

second metal/metal oxide nanoscale domain is needed, rather than a well-mixed metal alloy and metal oxides [21, 22]. The HRTEM images of the Pt–WO_3 particles here support such a possibility.

Further electrochemical experiments confirmed the conclusions from CV experiments. Figure 6 shows the chronoamperometric responses of different electrodes at 0.65 V vs Ag/AgCl. This applied potential is high and beyond the normal range of the operating potential of a DMFC. This high potential was used to generate sufficient current on the electrodes which have low Pt loadings and for better differentiation of the various electrodes activity. A comparison of constant-potential results follows the same trend as the CV results. The steady-state oxidation currents for the different electrodes are in the order 1 : 1 > 3 : 1 > 1 : 3, whereas the 1 : 2 and Etek Pt : Ru results are similar to the 3 : 1 result. Finally, chronopotentiograms of the electrodes, except the Etek electrode, were performed at a current density of 10 mA cm^{-2} and with a higher loading of 0.3 mg Pt cm^{-2}. This Pt loading is compatible with the expected value for viable commercial applications of DMFC. As shown in figure 7, the same trend of activity is observed with 1 : 1 Pt : W giving the best activity and lowest steady-state oxidation potential.

With the glycol synthesis of Pt–WO_3 nanoparticles, the activity of Pt–WO_3 was investigated here with better uniformity and control of Pt : W and size at nanoscales, as opposed to earlier studies. The XPS and TEM characterizations also gave addition insights into the chemical and physical state of Pt and W and their roles in electro-oxidation of methanol. We fall short, however, of thorough XPS, HRTEM, and other characterizations, e.g. TEM-EDX of Pt–WO_3 nanoparticles for all Pt : W ratios. The correlation of such data to activity at different compositions should warrant better understanding of the mechanism of methanol oxidation and how it is affected by the

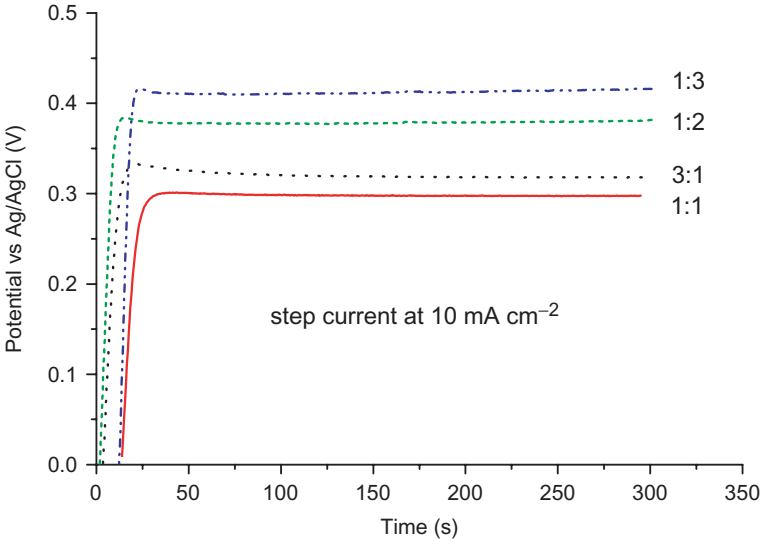

Figure 7. Chronopotentiograms of methanol oxidation at 10 mA cm^{-2} in 0.5 M methanol + 0.5 M H_2SO_4 at room temperature for different compositions of Pt–WO_3 nanoparticles at the same loading of 0.3 mg Pt cm^{-2}. This figure is available in colour online.

nanocomposition and structure of the catalyst. It is also necessary to compare with other platinum-based nanoparticles, e.g. Pt–Ru, prepared with similar control of nanosize and nanocomposition in order to develop better catalysts for low-temperature fuel cells.

4. Conclusions

The synthesis of Pt–WO_3 by the glycol method is simple and effective. It gives good control of composition and size at the nanometre scale while the synthesis allows straightforward scale-up for low-cost commercial production. Electrocatalytic activities of Pt–WO_3 nanoparticles for methanol oxidation revealed an optimum ratio of 1 : 1 in Pt : W, when Pt is mostly in metallic form while W has an oxidation state of +6. The observation of some cubic packing nanodomains in HRTEM suggests the possibility of physical aggregation of WO_3 with Pt in the nanoscale domains. The performance of Pt–WO_3 can be competitive with Pt–Ru as observed in the comparison of a commercial catalyst at equal loading of Pt.

Acknowledgements

This work was supported by grants HKU 7072/01P and HKU 7005/03P awarded by the Research Grants Council of Hong Kong. The XPS analysis was performed at CSAR in Hong Kong Baptist University.

References

[1] K. Y. Chan, J. Ding, J. Ren, S. A. Cheng, and K. Y. Tsang. Supported mixed metal nanoparticles for fuel cell electrode. J. Mater. Chem. **14**, 505 (2004).
[2] Z. D. Wei and S. H. Chan. Electrochemical deposition of PtRu on an uncatalyzed carbon electrode for methanol electrooxidation. J. Electroanal. Chem. **569**, 23 (2004).
[3] A. N. Haner and P. N. Ross. Electrochemical oxidation of methanol on tin-modified platinum single-crystal surfaces. J. Phys. Chem. **95**, 3740 (1991).
[4] T. Kim, M. Takahashi, M. Nagai, and K. Kobayashi. Methanol electrooxidation on carbon-supported Pt_3Ru_2Sn ternary catalyst. Chem. Lett. **33**, 478 (2004).
[5] S. Wasmus and A. Küver. Methanol oxidation and direct methanol fuel cells: a selective review. J. Electroanal. Chem. **461**, 14 (1999).
[6] B. D. McNicol, D. A. J. Rand, and K. R. Williams. Direct methanol–air fuel cells for road transportation. J. Power Sources **83**, 15 (1999).
[7] P. K. Shen and A. C. C. Tseung. Co-deposited $Pt–WO_3$ electrodes 1. Methanol oxidation and in-situ FTIR studies. J. Electrochem Soc. **4**, 3082 (1994).
[8] R. S. A. Babu, S. S. Murthy, and B. Viswanathan. Electrocatalytic oxidation of methanol on platinum based catalysts. Studies Surf. Sci. Catal. **113**, 787 (1998).
[9] X. Zhang, K.-Y. Chan, J. K. You, Z. G. Lin, and A. C. C. Tseung. Partial oxidation of glucose by Pt/WO_3 electrode. J. Electroanal. Chem. **430**, 1473 (1997).
[10] X. Zhang, K.-Y. Chan, and A. C. C. Tseung. Electrochemical oxidation of glucose by Pt/WO_3 electrode. J. Electroanal. Chem. **386**, 241 (1995).
[11] X. Zhang and K.-Y. Chan. Microemulsion synthesis and electrocatalytic properties of platinum–ruthenium nanoparticles. Chem. Mater. **15**, 451 (2003).
[12] J. Ding, K.-Y. Chan, J. Ren, and F.-S. Xiao. Platinum and platinum–ruthenium nanoparticles supported on ordered mesoporous carbon and their electrocatalytic performance for fuel cell reactions. Electrochimica Acta **50**, 3131 (2005).
[13] Z. Sun, H. C. Chiu, and A. C. C. Tseung. Oxygen reduction on Teflon bonded $Pt/WO_3/C$ electrode in sulfuric acid. Electrochem. Solid State Lett. **4**(3), E9 (2001).
[14] F. S. Hoor, M. F. Ahmed, and S. M. Mayanna. Methanol oxidative fuel cell: electrochemical synthesis and characterization of low-priced WO3–Pt anode material. J. Solid State Electrochem. **8**, 572 (2004).
[15] K. W. Park, K. S. Ahn, J. H. Choi, Y. C. Nah, Y. M. Kim, and Y. E. Sung. $Pt–WO_x$ electrode structure for thin-film fuel cells. Appl. Phys. Lett. **81**, 907 (2002).
[16] C. W. Chen, T. Serizawa, and M. Akashi. Preparation of platinum colloids on polystyrene nanospheres and their catalytic properties in hydrogenation. Chem. Mater. **11**, 1381 (1999).
[17] D. V. Goia and E. Matijevic. Tailoring the particle size of monodispersed colloidal gold. Colloids Surf. A **146**, 13 (1999).
[18] Y. Wang, J. Ren, K. Deng, L. Gui, and Y. Tang. Preparation of tractable platinum, rhodium, and ruthenium nanoclusters with small particle size in organic media. Chem. Mater. **12**, 1622 (2000).
[19] X. Zhang, K. Y. Tsang, and K. Y. Chan. Electrocatalytic properties of supported platinum–cobalt nanoparticles with uniform and controlled composition. J. Electroan. Chem. **573**, 1 (2004).
[20] Z. X. Lu, S. M. Kanan, and C. P. Tripp. Synthesis of high surface area monoclinic WO_3 particles using organic ligands and emulsion based methods. J. Mater. Chem. **12**, 983 (2002).
[21] G. Gu, B. Zheng, W. Q. Han, S. Roth, and J. Liu. Tungsten oxide nanowires on tungsten substrates. Nano Lett. **2**(8), 849 (2002).
[22] X. L. Li, J. F. Liu, and Y. D. Li. Large-scale synthesis of tungsten oxide nanowires with high aspect ratio. Inorg. Chem. **42**, 921 (2003).
[23] J. M. Leger. Preparation and activity of mono- or bi-metallic nanoparticles for electrocatalytic reactions. Electrochimica Acta **50**(15), 3123 (2005).
[24] F. Liu, J. Y. Lee, and W. J. Zhou. Template preparation of multisegment PtNi nanorods as methanol electro-oxidation catalysts with adjustable bimetallic pair sites. J. Phys. Chem. B **108**(46), 17959 (2004).
[25] C. D. Wagnew, W. M. Riggs, L. E. Davies, and J. F. Mouder. *Handbook of X-ray Photoelectron Spectroscopy*, Perkin-Elmer, Eden Prairie, MN (1978).
[26] K. W. Park, J. H. Choi, B. K. Kwon, S. A. Lee, Y. E. Sung, H. Y. Ha, S. A. Hong, H. Kim, and A. Wieckowski. Chemical and electronic effects of Ni in Pt/Ni and Pt/Ru/Ni alloy nanoparticles in methanol electrooxidation. J. Phys. Chem. B. **106**, 1869 (2002).
[27] R. J. Colton and J. W. Rabalais. Electronic-structure of tungsten and some of its borides, carbides, nitrides, and oxides by X-ray electron-spectroscopy. Inorg. Chem. **15**, 236 (1976).